



A Journal of the Gesellschaft Deutscher Chemiker

Angewandte Chemie

GDCh

International Edition

www.angewandte.org

Accepted Article

Title: Unexpected Chromophore-Solvent Reaction Leads to Bicomponent Aggregation-Induced Phosphorescence

Authors: Guoqing Zhang, Biao Chen, Wenhuan Huang, Hao Su, Hui Miao, and Xuepeng Zhang

This manuscript has been accepted after peer review and appears as an Accepted Article online prior to editing, proofing, and formal publication of the final Version of Record (VoR). This work is currently citable by using the Digital Object Identifier (DOI) given below. The VoR will be published online in Early View as soon as possible and may be different to this Accepted Article as a result of editing. Readers should obtain the VoR from the journal website shown below when it is published to ensure accuracy of information. The authors are responsible for the content of this Accepted Article.

To be cited as: *Angew. Chem. Int. Ed.* 10.1002/anie.202000865
Angew. Chem. 10.1002/ange.202000865

Link to VoR: <http://dx.doi.org/10.1002/anie.202000865>
<http://dx.doi.org/10.1002/ange.202000865>

Unexpected Chromophore-Solvent Reaction Leads to Bicomponent Aggregation-Induced Phosphorescence

Biao Chen,^[a] Wenhuan Huang,^[a] Hao Su,^[a] Hui Miao,^[a] Xuepeng Zhang*^[a] and Guoqing Zhang*^[a]

Abstract: Organic luminogens with persistent room-temperature phosphorescence (RTP) have found a wide range of applications in sensing, bioimaging, illumination, and information encryption. However, many RTP luminogens are prone to severe quenching in the crystalline state. Herein we report a working strategy to construct a donor- sp^3 -acceptor type of luminogen which exhibits aggregation-induced emission (AIE) while the donor- sp^2 -acceptor counterpart structure exhibits non-emissive solid state. Unexpectedly, it was discovered that a trace amount (0.01%) of structurally similar derivative, produced by a side reaction with the DMF solvent, could induce strong RTP with an absolute RTP yield up to 25.4% and a lifetime of 48 ms, although the identified substance does not show RTP by itself. Single-crystal XRD-based calculations suggest that $n-\sigma^*$ orbital interactions as a result of structural similarity may be responsible for the strong RTP in the bicomponent system. The current study provides a new insight into the design of multi-component, solid-state RTP materials from organic molecular systems.

Purely organic RTP materials are important for practical applications such as biological imaging and sensing,^[1] information encryption^[2] and flexible organic light-emitting diode (OLED) devices.^[3] Most of these applications require that these RTP molecules be utilized in the solid state since mobile phases usually dissipate the triplet excited state via various quenching mechanisms such as intramolecular rotations, biomolecular collisions and electron transfer.^[4] Consequently, organic RTP molecules are commonly used as molecular solids (e.g., crystals,^[5] films^[6]) or dopant^[7] in solid-state matrices such as polymers.^[8] In the latter case, deoxygenation can be a nuisance if the matrix is porous enough to allow gas diffusion;^[9] in this regard, crystalline materials are better suited media for harvesting RTP^[10] since they are usually gas-impermeable. Unfortunately, many molecules that exhibit long-lived RTP in polymers are prone to ACQ in aggregated forms such as the non-doped OLED emitting layer.^[11] To solve the conundrum, AIE^[12] materials are frequently designed. Structurally, AIE molecules often exhibit large rotational and vibrational freedoms which facilitate the radiationless transitions from the excited state to the ground state. Upon aggregation, such freedoms are reduced without inducing additional non-radiative transition (e.g., strong π stacking) modes so that the excited state energy is better preserved for emissive decay.^[13] For most organic luminogens, a common characteristic is the extended π

conjugation which renders the system planarity and rigidity, a good recipe for ACQ. In light of this problem, we recently proposed an AIE molecular motif that uses an sp^3 -type of linker to attach π -conjugated donor and acceptor together, which diminishes the sp^3 single-bond rotation but concomitantly prevents close molecular packing as aggregates.^[14] In the course of working with these molecular systems, we discovered that 5-bromo-2-(3,4-dimethoxybenzyl)isoindoline-1,3-dione (**BrPID**, Figure 1a) appeared to possess unusual solvent-dependent RTP, i.e., **BrPID** procured from DMF has very strong RTP which is absent when EtOH is used. The observed anomaly intrigued further investigation and was unveiled as a result of a side reaction from DMF and the AIEgen. More strangely, the side product, identified as an amino derivative of **BrPID**, lacks or shows very weak phosphorescence even at 77 K in other media including heavily brominated solvents. Herein, we present the discovery of the bicomponent AIE-RTP phenomenon, as well as experimental evidence for a plausible mechanism involving specific orbital interactions due to structural similarity, which can be illuminating for the rational design of solid-state organic RTP systems.

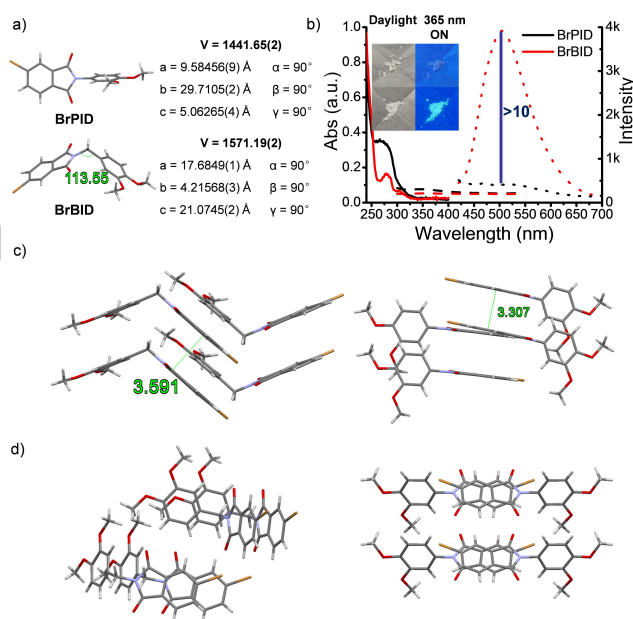


Figure 1. a) Stick models showing sp^2 - and sp^3 - carbon-linked phthalimide organic donor-acceptor structures with crystal lattice parameters. b) UV absorption spectra of **BrPID** and **BrBID** in mTHF (3×10^{-5} M) at 298 K (solid lines), PL spectra of **BrPID** and **BrBID** in mTHF (3×10^{-5} M) at 298 K (dash lines, $\lambda_{\text{ex}} = 280$ nm), PL spectra of **BrPID** and **BrBID** in the solid state in air at 298 K (dot lines, $\lambda_{\text{ex}} = 365$ nm), inset: Photographs of **BrPID** (up row) and **BrBID** at daylight and 365 nm irradiation ON. c) SC-XRD showing $\pi-\pi$ stacking distances and d) phthalimide ring overlaps for **BrBID** (left) and **BrPID** (right).

[a] Dr. B. Chen, Mr. W. Huang, Mr. H. Su, Prof. H. Miao, Dr. X. Zhang, Prof. G. Zhang
Hefei National Laboratory for Physical Science at the Microscale,
University of Science and Technology of China, 96 Jinzhai Rd,
Hefei, Anhui 230026 (China)
E-mail: zhangxp@ustc.edu.cn
gzhang@ustc.edu.cn

Supporting information for this article is given via a link at the end of the document.

Two sp^2 - and sp^3 -carbon-linked donor-acceptor phthalimide molecules **BrPID** (P for phenyl) and **BrBID** (B for benzyl), shown

in Figure 1a, were facilely synthesized in high yields by a single-step amine-anhydride condensation reaction in ethanol (Scheme S1). The target compounds were confirmed by ^1H and ^{13}C nuclear magnetic resonance (NMR) spectra and high resolution mass spectrometry (HRMS), elemental analysis (EA) and high performance liquid chromatography (HPLC, Figure S1, Figure S15-S20). Single-crystal X-ray diffraction (SC-XRD, Figure 1a) reveals that the dihedral angle between the donor and acceptor planes is 113.55° imposed by the tetrahedral geometry of the $sp^3\text{-CH}_2\text{-}$ group; the sp^2 counterpart has nearly perpendicular planes. These configuration differences caused by bonding manners have a profound impact on the photophysical properties of the two molecules. The absorption and emission spectra in dilute 2-methyl-tetrahydrofuran (m-THF, 30 μM) are presented in Figure 1b, along with the solid state emission spectra (dot lines). The main absorption band lies mainly < 350 nm for both **BrPID** and **BrBID** ($\lambda_{\text{max}} = 280$ and 278 nm, respectively). When excited at the absorption maxima for both molecules, no discernible fluorescence could be recorded (Figure 1b, $\Phi_{\text{PL}} < 0.001$) at 298 K. In the solid state, under the irradiation of a hand-held UV lamp, however, bright green-blue photoluminescence of **BrBID** ($\lambda_{\text{em}} = 505$ nm, $\tau = 0.49$ μs) could be easily observed by the naked eye while **BrPID** was not fluorescent at all. Consequently, **BrBID** exhibits typical AIE features. There is no obvious difference in the degree of crystallinity according to the powder XRD data (Figure S3). Hence, one can speculate that it is likely due to the way in which molecules stack. From XRD data (Table S1, Figure 1c and 1d), the phthalimide ring stacking distances are 3.307 \AA for **BrPID** and 3.591 \AA for **BrBID**, respectively, consistent with the hypothesis that sp^3 -linkers tend to hinder tight molecular packing, which explains the solid-state quenching^[15] and AIE behaviors^[16] for the two analogs, respectively.

In the process of optimizing the product yield, two working solvents, ethanol and DMF, were employed (see Supporting Information, SI). Surprisingly, **BrBID** synthesized from DMF (**1**) emitted strong yellow photoluminescence (PL, Figure 2a, $\lambda_{\text{em}} = 565$ nm with a 506-nm shoulder band) with intense delayed emission under the irradiation of 365-nm UV light, while **2** (synthesized from EtOH) showed an identical emission profile to that of ultra-purified **BrBID** (Figure 1b and 2a, $\lambda_{\text{em}} = 506$ nm). At a closer examination, time-correlated spectroscopy ($\Delta t = 0.05$ ms) revealed that for **1** the prompt and delay emission spectra are nearly identical with a lifetime of 45.3 ms (Figure 2b), indicating that **1** has nearly pure RTP emission. The RTP quantum yield is measured to be >0.20 for crystals extracted from the particular reaction condition. Sample **2**, nevertheless, has a mixed excited state given the Br presence that enhances the spin-orbit coupling ($\tau_{@506\text{nm}} = 0.49$ μs) due to the internal heavy-atom effect. The phenomenon was first proposed as a result of solvent-dependent polymorph, i.e., crystallizations from different solvents yield different molecular packings (Figure S3).^[17] However, **1** repeatedly recrystallized with either EtOH or DMF still showed strong RTP ~ 560 nm, but with varied intensities (relative to the 506-nm band) and durations, which prompted us to consider an impurity giving off RTP. After purification via silica gel chromatography ($2\times$), the strong RTP at 560 nm disappeared (and showed the same luminescence properties as those for ultrapure **BrBID**, Figure S4). These

results clearly demonstrated that an unknown RTP emitter is involved.

We then employed HPLC to analyze the components of different samples by monitoring the onset absorptions at both 280 and 365 nm, where several small impurity peaks were uncovered gradually when the acetonitrile-water ratio was optimized from 100/0 to 55/45 (v/v, Fig. S5, note that the solvent ratio optimization is essential because impurity information is easily buried by the absorption of the dominant **BrBID**, should acetonitrile be used as the sole eluent). Although **1** and **2** had several peaks ranging from $\sim 0.1\%$ to $\sim 1\%$ (relative to **BrBID**), the top priority was given to a peak unique to sample **1** (Figure S6, elution time = 8.3 min). After repeated chromatograph purifications from a large batch of reaction (~ 100 g scale), sufficient impurity **X** (> 50 mg) was isolated. The structure of **X** was determined by ^1H NMR, ^{13}C NMR, HPLC and HRMS (Figure S21-S23), and was also analyzed with SC-XRD (Figure 2c, S24 and table S2) as a derivative of **BrBID**, which has previously been discovered as a by-product from DMF and aryl halide.^[18] The photophysical properties of **X** are also shown in Figure 2c. It was found that **X** is fluorescent in both liquid solvent and as crystals (Figure S7). However, no emission longer than a few nanoseconds could be recorded even at 77 K in any form, indicating rather weak triplet state activities of **X** without **BrBID** presence. In order to confirm that the RTP of sample **1** is indeed from **X** doping, photoluminescence spectra were compared for the bicomponent crystal of **X/BrBID** (0.05% m/m) and sample **1**, respectively. As shown in Figure 2d, the two materials possess almost identical prompt and delayed spectra. Furthermore, time-resolved emission decay curves indicate that they have almost the same lifetime (48.1 ms for **X/BrBID**), which confirms the identity of **X** as the persistent RTP emitter in sample **1**.

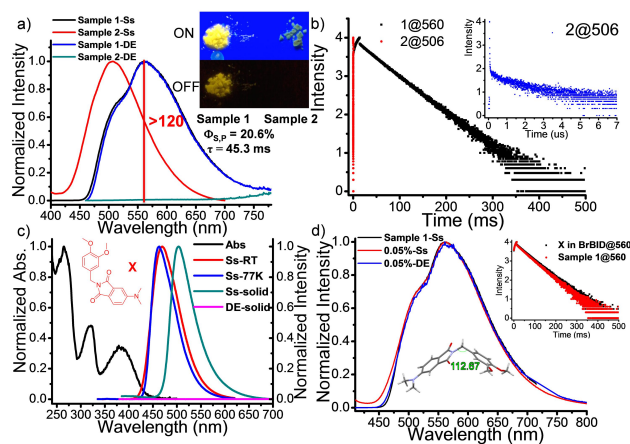


Figure 2. a) Steady-state PL spectra (Ss) and delayed ($\Delta t = 0.05$ ms) emission spectra (DE) of **1** and **2** in the solid state at 298 K ($\lambda_{\text{ex}} = 365$ nm). b) Emission decay curves of **1** and **2** at 560 nm and 506 nm in solid-state. c) Steady-state PL spectra of **X** in mTHF (3×10^{-5} M) at 298 K and 77 K ($\lambda_{\text{ex}} = 320$ nm), steady state PL and delayed ($\Delta t = 0.05$ ms) spectra of **X** in solid state at 298 K ($\lambda_{\text{ex}} = 365$ nm). d) SC-XRD of **X**, steady-state PL spectra and delayed ($\Delta t = 0.05$ ms) spectra of 0.05% **X** dopant in **BrBID** and sample **1** in the solid state at 298 K ($\lambda_{\text{ex}} = 365$ nm); inset: emission decay curves of samples **1** and **X** monitored at 560 nm.

To find out how **X**-doping correlates with RTP in **Br**BID, we blended **Br**BID with different proportions of **X** ranging from 0.01% to 5% (by mass fraction, Figure 3b and S8) in dichloromethane. By solution evaporation of the mixture solution homogenous bicomponent crystals (with no observable phase separations) could be obtained possibly owing to the very similar molecular structures of **X** and **Br**BID. Surprisingly, with only 0.01% **X** presence (when **X** does not even show up on HPLC spectrum), strong yellow RTP with an afterglow was observed by the naked eye, which implies that the doping efficacy is exceedingly high. Under spectroscopic investigation, all samples exhibit strong yellow RTP bands centered at ~560 nm except for the sample with 0.01% **X** doping, which has more intense shoulder emission at ~506 nm, ascribed to the bulk **Br**BID luminescence. The highest PL intensity was recorded for 1% **X** doping with an absolute RTP quantum yield >0.25. Correspondingly, **Br**BID crystals prepared from DMF terminated at different reactions times (1h, 4h, 12h and 24h), and were also examined by spectroscopy (Figure 3c and Figure S9). While the 1-h sample is barely phosphorescent, the 4h- and 12h-samples show highly efficient RTP. The **X** content increases gradually as the reaction proceeds (Figure S10, HPLC), and the 24h-sample shows white emission and bears a new band centered at ~490 nm, attributed to the bulk luminescence of phase-separated **X** crystals (by comparing with Figure 2c). In this sense, the reaction time may be used to tune the concentration of **X** and thus the luminescence properties of the resulted materials. Finally, it was also discovered that persistent mechanoluminescence^[19] (ML) emanating from **X**/**Br**BID (e.g., sample **1**) could be observed at room

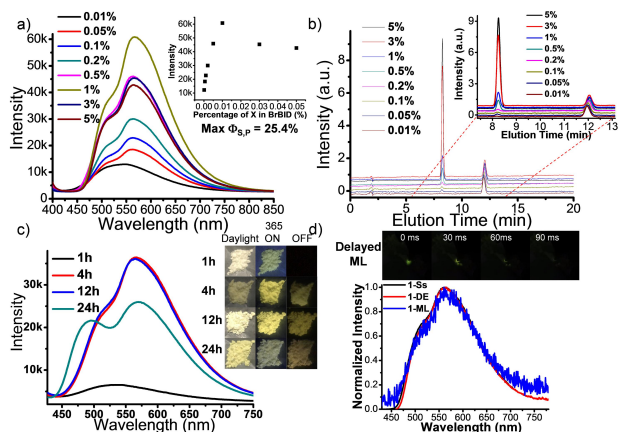


Figure 3. a) Steady-state PL spectra of **X** dopants (0.01%, 0.05%, 0.1%, 0.2%, 0.5%, 1%, 3% and 5%) in **Br**BID crystals at 298 K ($\lambda_{ex} = 365$ nm); inset: PL intensity at 560 nm vs. doping content. b) HPLC spectra monitored at the onset absorption of 365 nm for different dopant ratios. c) PL spectra of crude **Br**BID products from different reaction times in DMF; inset: photographs of crude products in daylight and under 365-nm irradiation. d) ML images and ML spectrum of sample **1** taken at room temperature.

temperature. When the crystals were crushed with various forms of mechanical force, persistent yellow luminescence with a duration of ~0.1 s was observed without external light excitation. The ML was so strong that it was observable even in daylight

and the recorded ML spectrum of **1** (Figure 3d) superimposes with that of the photoluminescence. To date, the most accepted explanation for ML is excitation through electrification,^[20] in which case the **X**/**Br**BID molecules are driven into charge-separated excited states via electrical field instead of electromagnetic field.

As for the RTP-activation mechanism by **X** doping, the external heavy-atom effect (i.e., Br on **Br**BID in close contact with **X**) is highly conducive. However, if such a hypothesis were true, then doping the sp^2 carbon-connected **Br**PID with **X** should result in similar RTP given that the bromine atoms were mainly responsible. When **X** was blended with **Br**PID under the same condition (as **Br**BID), no RTP was observed at all (Figure S11); when **X** was dissolved in 1,6-dibromohexane, extremely weak phosphorescence was recorded (Figure S12), excluding the possibility of external heavy-atom influence alone. Based on these experimental observations, we proposed a plausible model (Figure 4) for the highly efficient RTP, aided by theoretical calculations, which concerns where the **X** molecule fits after doping. For **Br**BID crystals, **X** only differs in the 2-substitution on the phthalimide ring, which implies that as long as the interaction between C-Br and C-NMe₂ is not repulsive, the **X** molecule has a large probability to spatially replace a **Br**BID molecule in the crystal lattice. Given that the emission spectrum exhibits vibronic features which indicate localized Frenkel or charge-transfer excitons, using the dimer coordinates derived from the SC-XRD, we tried two different methods: 1) arbitrarily replace one C-Br with C-NMe₂ group with fixed **Br**BID coordinates; 2) optimization of the dimer energy built upon SC-XRD coordinates for **X** and **Br**BID. Both methods of calculations, employing molecular orbital (MO, Figure 4 left) and natural bond orbital (NBO, Figure 4 right) models, suggest that there is orbital interaction between the two groups in that the σ^* (C-Br) and possibly the π^* spatially overlap with that of the lone pair electrons on -NMe₂.^[21] The findings have two major implications: 1) the **X** molecule should be held even stronger when it replaced a **Br**BID molecule; 2) with **X** molecules being the absolute minority species in the bicomponent crystal, the -NMe₂ non-bonding orbital is shared by two C-Br σ^* orbitals. Since the excited state heavily involves the -NMe₂ participation (Figure S25), the spin-orbit coupling should be enhanced for **X** in the bicomponent crystal due to such external heavy atom effect.

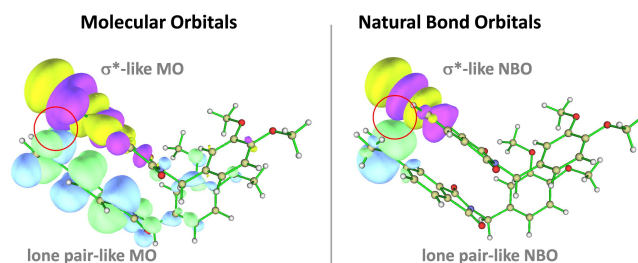


Figure 4. Molecular orbital (MO, left) and natural bond orbital (NBO, right) models demonstrate orbital overlaps between an unoccupied σ^* (C-Br) like orbital with an occupied lone pair-like (-NMe₂) one.

In summary, we have constructed an AIE luminogen, **BrBID**, by an sp^3 methylene linker, which exhibits short-lived RTP (μs -long) with an emission maximum at 506 nm. An unexpected side-reaction between the DMF solvent and **BrBID** results in an amino derivative **X** which induces intense ($\Phi = 25.4\%$) and substantially prolonged ($\tau = 48$ ms) RTP in the **X-in-BrBID** bicomponent solids. The impurity **X** was carefully isolated and resolved by SC-XRD. It was found that the intense RTP of **X** was only activated by the **BrBID** matrix and was explained in terms of specific molecular orbital interactions from SC-XRD and theoretical calculations. The current discovery sets an important example for designing bicomponent organic RTP systems.

Acknowledgements

We thank the National Key R&D Program of China (2017YFA0303500 to G. Z. and Y. L.), the National Natural Science Foundation (GG2340000364 to G. Z.) and the Fundamental Research Funds for the Central Universities (WK2340000068 to G. Z.).

Conflict of interest

The authors declare no conflict of interest.

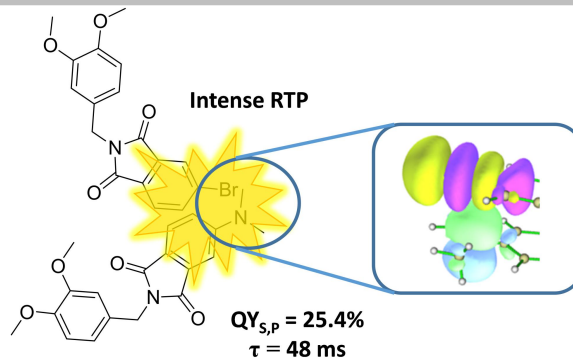
Keywords: aggregation-induced emission • room temperature phosphorescence • chromophore-solvent reaction • sp^3 linked donor-acceptor • persistent mechanoluminescence

- [1] a) M. S. Kwon, D. Lee, S. Seo, J. Jung, J. Kim, *Angew. Chem. Int. Ed.* **2014**, *53*, 11177–11181; *Angew. Chem.* **2014**, *126*, 11359–11363. b) X. Chen, C. Xu, T. Wang, C. Zhou, J. Du, Z. Wang, H. Xu, T. Xie, G. Bi, J. Jiang, *Angew. Chem. Int. Ed.* **2016**, *55*, 9872–9876. *Angew. Chem.* **2016**, *128*, 10026–10030.
- [2] a) W. Zhao, Z. He, J. W. Lam, Q. Peng, H. Ma, Z. Shuai, G. Bai, J. Hao, B. Z. Tang, *Chem* **2016**, *1*, 592-602; b) L. Bian, H. Shi, X. Wang, K. Ling, H. Ma, M. Li, Z. Cheng, C. Ma, S. Cai, Q. Wu, N. Gan, X. Xu, Z. An, W. Huang, *J. Am. Chem. Soc.* **2018**, *140*, 10734-10739.
- [3] S. Hirata, *Adv. Opt. Mater.* **2017**, *5*, 1700116.
- [4] G. Baryshnikov, B. Minaev, H. Ågren, *Chem. Rev.* **2017**, *117*, 6500-6537.
- [5] H. Wu, W. Chi, G. Baryshnikov, B. Wu, Y. Gong, D. Zheng, X. Li, Y. Zhao, X. Liu, H. Ågren, *Angew. Chem. Int. Ed.* **2019**, *58*, 4328–4333; *Angew. Chem.* **2019**, *131*, 4372–4377.
- [6] M. S. Kwon, Y. Yu, C. Coburn, A. W. Phillips, K. Chung, A. Shanker, J. Jung, G. Kim, K. Pipe, S. R. Forrest, *Nat. Commun.* **2015**, *6*, 8947.
- [7] a) R. Kabe, C. Adachi, *Nature* **2017**, *550*, 384-387. b) Q. Li, M. Zhou, Q. Yang, Q. Wu, J. Shi, A. Gong, M. Yang, *Chem. Mater.* **2016**, *28*, 8221-8227.
- [8] N. Gan, H. Shi, Z. An, W. Huang, *Adv. Funct. Mater.* **2018**, *28*, 1802657.
- [9] G. Zhang, G. M. Palmer, M. W. Dewhurst, C. L. Fraser, *Nat. Mater.* **2009**, *8*, 747.
- [10] X. Zhang, L. Du, W. Zhao, Z. Zhao, Y. Xiong, X. He, P. F. Gao, P. Alam, C. Wang, Z. Li, *Nat. Commun.* **2019**, *10*, 1-10.
- [11] T. Wang, X. Su, X. Zhang, X. Nie, L. Huang, X. Zhang, X. Sun, Y. Luo, G. Zhang, *Adv. Mater.* **2019**, 1904273.
- [12] Y. Hong, J. W. Lam, B. Z. Tang, *Chem. Soc. Rev.* **2011**, *40*, 5361-5388.
- [13] R. T. Kwok, C. W. Leung, J. W. Lam, B. Z. Tang, *Chem. Soc. Rev.* **2015**, *44*, 4228-4238.
- [14] a) B. Chen, X. Zhang, Y. Wang, H. Miao, G. Zhang, *Chem. Asian J.* **2019**, *14*, 751-754. b) L. Huang, B. Chen, X. Zhang, C. O. Trindle, F. Liao, Y. Wang, H. Miao, Y. Luo, G. Zhang, *Angew. Chem. Int. Ed.* **2018**, *57*, 16046–16050; *Angew. Chem.* **2018**, *130*, 16278–16282. c) W. Huang, X. Zhang, B. Chen, H. Miao, C. O. Trindle, Y. Wang, Y. Luo, G. Zhang, *Chem. Commun.* **2019**, *55*, 67-70.
- [15] W. Z. Yuan, P. Lu, S. Chen, J. W. Lam, Z. Wang, Y. Liu, H. S. Kwok, Y. Ma, B. Z. Tang, *Adv. Mater.* **2010**, *22*, 2159-2163.
- [16] E. G. McRae, M. Kasha, *J. Chem. Phys.* **1958**, *28*, 721-722.
- [17] J. A. Li, J. Zhou, Z. Mao, Z. Xie, Z. Yang, B. Xu, C. Liu, X. Chen, D. Ren, H. Pan, *Angew. Chem. Int. Ed.* **2018**, *57*, 6449–6453; *Angew. Chem.* **2018**, *130*, 6559-6563.
- [18] J. Muzart, *Tetrahedron* **2009**, *65*, 8313-8323.
- [19] Y. Xie, Z. Li, *Chem* **2018**, *4*, 943-971.
- [20] G. E. Hardy, J. C. Baldwin, J. I. Zink, W. C. Kaska, P. H. Liu, L. Dubois, *J. Am. Chem. Soc.* **1977**, *99*, 3552-3558.
- [21] X. Sun, B. Zhang, X. Li, C. O. Trindle, G. Zhang, *J. Phys. Chem. A* **2016**, *120*, 5791-5797.

Entry for the Table of Contents

COMMUNICATION

Trace impurity by unexpected solvent-chromophore reaction leading to highly efficient room-temperature phosphorescence.



Biao Chen, Wenhuan Huang,
Hao Su, Hui Miao, Xuepeng
Zhang* and Guoqing Zhang*

Page No. – Page No.

Unexpected Chromophore-Solvent Reaction Leads to Bicomponent Aggregation-Induced Phosphorescence